

Above-barrier resonant transitions in $\text{Al}_x\text{Ga}_{1-x}\text{As}/\text{AlAs}/\text{GaAs}$ heterostructures

Marcello Colocci, Juan Martinez-Pastor,* and Massimo Gurioli

*European Laboratory for Non Linear Spectroscopy and Department of Physics, University of Florence,
Largo Enrico Fermi 2, 50125 Firenze, Italy*

(Received 5 March 1993)

In this work we demonstrate the existence of above-barrier quasibound states in $\text{Al}_{0.3}\text{Ga}_{0.7}\text{As}/\text{AlAs}/\text{GaAs}$ double-barrier quantum-well structures, by using both continuous-wave and time-resolved photoluminescence techniques in addition to reflectivity measurements. A series of clearly resolved resonances is found in the optical spectra. Their energy positions agree fairly well with the energies found for the quasibound states when analyzing the density of states of the heterostructure continuous spectrum. As shown by the analysis of the envelope wave function these resonances are localized in the $\text{Al}_{0.3}\text{Ga}_{0.7}\text{As}$ barrier regions and are found to induce both an increase of the interband absorption and a reduction of the carrier capture efficiency into the wells.

I. INTRODUCTION

Band-gap engineering provides the possibility of controlling the electronic and optical properties of semiconductor quantum-well (QW) heterostructures by varying the layer thicknesses and material compositions. Several nonconventional structures have been proposed and realized for both investigating peculiar aspects of the confined carrier physics and improving the performances of QW devices.

In particular, $\text{Al}_x\text{Ga}_{1-x}\text{As}/\text{AlAs}/\text{GaAs}$ double-barrier quantum wells (DBQW's), where two thin barriers of AlAs are inserted on each side of the wells, have received increasing attention. Due to the insertion of the AlAs layers, the energy of the bound state within the well increases up to the continuum threshold for decreasing well width and eventually no bound states exist even in the case of relatively thick wells. This property makes the DBQW's ideal systems for analyzing the kinetics of carrier recombination from shallow subbands and several interesting properties have been recently reported. On one hand, an increase of the excitonic lifetime has been found, in agreement with the two-dimensional–three-dimensional (2D-3D) transition, due to the penetration of the carrier wave function into the barrier regions.¹ On the other hand, by varying the shallowness of the carrier subbands, the relevance of the carrier escape from the wells has been proved as an intrinsic thermally activated nonradiative channel.² Finally the transition between type-I and type-II exciton recombination, due to the crossing of the Γ bound state within the GaAs well and the X bound state inside the AlAs cladding barriers, has been demonstrated.³

At the same time, a new class of tunable infrared detectors based on intersubband absorption between GaAs QW bound states⁴ has spurred growing interest due to the high responsivity that can be obtained with *ad hoc* tailored QW structures. It has been suggested in recent papers^{5,6} that performances even higher than those ob-

tained in Ref. 4 can be reached when the transition involves bound to quasibound states inside the quantum well. In fact, it has been realized that resonances in the continuous spectrum can be present, in addition to the ordinary bound states, in DBQW's as well as in compositionally asymmetric QW's;^{7,8} increased oscillator strengths are predicted in these systems resulting in an increase of both the absorption coefficient and the responsivity of the device.

In this paper we report a detailed investigation, in a set of $\text{Al}_{0.3}\text{Ga}_{0.7}\text{As}/\text{AlAs}/\text{GaAs}$ DBQW's, of a different kind of extended states than in Ref. 8, namely, those originated in the barrier regions due to the presence of multiple DBQW's in the same sample. In fact, the analysis of the density of states (DOS) in these systems shows sharp resonances due to quasibound states in the $\text{Al}_{0.3}\text{Ga}_{0.7}\text{As}$ barrier regions, in close analogy with the well-known features of resonant tunneling structures. Direct evidence for the existence of extended resonant states above the $\text{Al}_{0.3}\text{Ga}_{0.7}\text{As}$ band-gap energy is provided by the experimental spectra [reflectivity and photoluminescence excitation (PLE)], where a series of peaks is clearly resolved. A fairly good agreement is obtained between the energy position of the optical transitions and the energy of the quasibound states found in the DOS. We also find that the presence of localized resonances in the $\text{Al}_{0.3}\text{Ga}_{0.7}\text{As}$ barrier region results in a sizable slowing down of the carrier capture process into the wells as demonstrated by the time-resolved photoluminescence (TRPL) measurements.

The paper is organized as follows. In Sec. II we characterize the continuous spectrum of the electronic states in DBQW's by a simple and general method based on the direct determination of the DOS. Section III is devoted to the description of the samples and the experimental setup. A discussion of the results is reported in Sec. IV and the concluding remarks are given in Sec. V. Finally the Appendix contains details of the model for determining the DOS.

II. DENSITY OF STATES IN THE CONTINUOUS SPECTRUM

Prominent features in the continuous spectrum of layered systems, such as the semiconductor QW's, can be obtained either by evaluating the change $\Delta\rho(E)$ in the DOS originated by the localized potential defining the heterostructures or by the calculation of the transmission probability $T(E)$. The general relationship between the two quantities has been recently demonstrated showing that the sharp resonances have the same position and width in both $\Delta\rho(E)$ and $T(E)$;⁹ nevertheless, $\Delta\rho(E)$ is a more general quantity to investigate because it is well defined even when $T(E)=0$.

Analytic expressions for $\Delta\rho(E)$ have been derived recently for some relevant potential profiles;¹⁰ indeed, for a localized perturbation within a flat potential, as it is in the case of DBQW's, one finds¹⁰

$$\Delta\rho(E) = \frac{1}{\pi} \frac{d\Phi(E)}{dE}, \quad (1)$$

where $\Phi(E)$ is the energy-dependent phase of the transmission amplitude $t(E)$ [$T(E)=|t(E)|^2$]. However, for nonconventional heterostructures the expression for $\Phi(E)$ can be complicated and the analytical derivation becomes quite lengthy, even if straightforward. Therefore it can be more useful to derive $\Delta\rho(E)$ by means of the simple numerical method, derived in Ref. 11 and applied to several important problems,^{11,12} which is based on the evaluation of the DOS for a large but finite system. The two methods (analytical and numerical) have been demonstrated to be perfectly equivalent¹⁰ and therefore the choice is only a matter of convenience.

Here we have used the numerical derivation, outlined in the Appendix, for the DBQW potential sketched in Fig. 1; the corresponding change in the electron DOS is reported in Fig. 2 for the design parameters of the samples investigated. A series of sharp peaks is found in $\Delta\rho(E)$; their energy positions agree fairly with those given by the condition

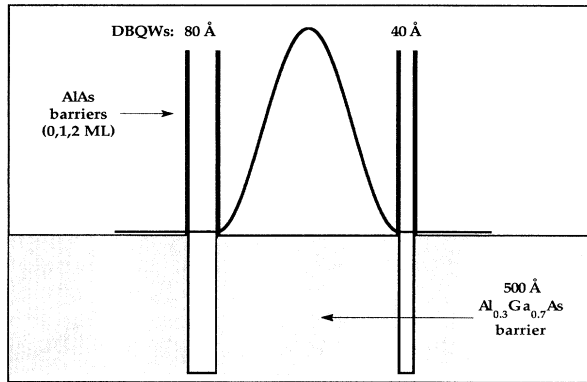


FIG. 1. Conduction-band profile for a multi-DBQW structure; the parameters in the figure refer to the structure for which $\Delta\rho(E)$ has been evaluated and shown in Fig. 2. The curve corresponds to the electron probability $|\Psi(z)|^2$ for the first quasibound state reported in Fig. 2(c).

$$E_n = \frac{1}{2m^*} \left[\frac{\pi\hbar}{L} n \right]^2 \quad (n=1,2,\dots) \quad (2)$$

corresponding to the energy of the n th bound state in an infinite well of thickness L equal to the width of the $\text{Al}_{0.3}\text{Ga}_{0.7}\text{As}$ barrier between the wells (here $L=500$ Å and $m^*=0.92m_0$, i.e., the electron effective mass of the alloy). We will therefore attribute the sharp resonances in $\Delta\rho(E)$ to quasibound states in the $\text{Al}_{0.3}\text{Ga}_{0.7}\text{As}$ region; in fact, due to the presence of multiple DBQW's in the same structure, the AlAs layers also clothe the $\text{Al}_{0.3}\text{Ga}_{0.7}\text{As}$ barrier between the wells and there is a strong similarity between this region and the well-known resonant tunneling structures.

The assignment is confirmed by the analysis of the wave function $\Psi(E)$ at the energies of the peaks in $\Delta\rho(E)$. As an example, $|\Psi(E)|^2$ at the energy corresponding to the first resonance in $\Delta\rho(E)$ is reported in Fig. 1 for the DBQW structure with two AlAs monolayers (ML's). Indeed we see that the wave function approximately vanishes at the AlAs interface and, moreover, that $|\Psi(E)|^2$ is strongly localized within the $\text{Al}_{0.3}\text{Ga}_{0.7}\text{As}$ barrier region.

The wave functions of the higher-energy quasibound states reported in Fig. 2 have similar properties; however, corresponding to excited levels ($n>1$) inside the infinitely deep well, they show $n-1$ nodes inside the $\text{Al}_{0.3}\text{Ga}_{0.7}\text{As}$ barrier. At the same time, it should be noted that at higher energies than reported in Fig. 2 one

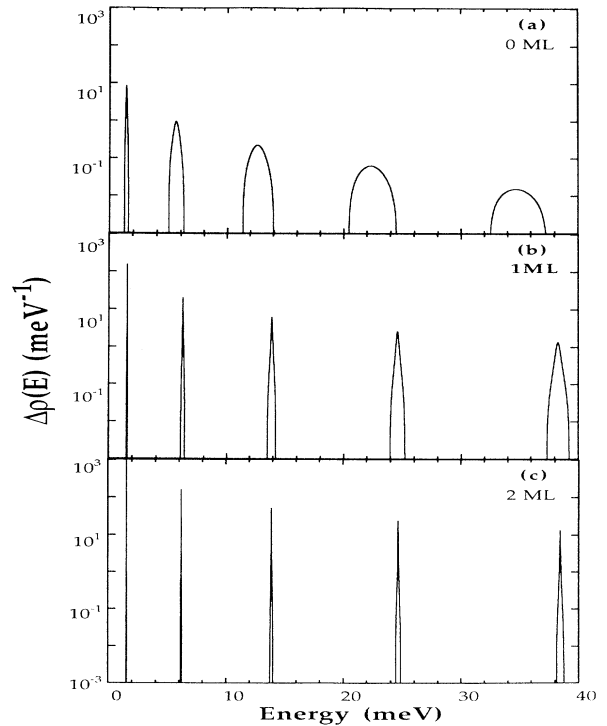


FIG. 2. Change in the electron DOS for the structure reported in Fig. 1; (a) 0-ML, (b) 1-ML, and (c) 2-ML structures. The energies are measured from the bottom of the $\text{Al}_{0.3}\text{Ga}_{0.7}\text{As}$ conduction band.

finds resonances in $\Delta\rho(E)$ associated to electron localization within the GaAs wells, as predicted in Ref. 8. As an example, for the DBQW's we refer to in Fig. 2, the first of such resonances is found around 230 meV and corresponds to a quasibound state mainly localized inside the 80-Å well. The study of this further kind of structure in the continuous spectrum is, however, outside the purpose of this paper.

The resonances in $\Delta\rho(E)$ reported in Fig. 2 broaden increasing their energy. The linewidth of the quasibound states is obviously related to the wave-function localization: the sharper the peak is in $\Delta\rho(E)$, the more localized the corresponding quasibound state is in the $\text{Al}_{0.3}\text{Ga}_{0.7}\text{As}$ region. Therefore, increasing the energy, the quasibound states become more and more delocalized. We also find that the sharp resonances in $\Delta\rho(E)$ have a Lorentzian line shape with unit area, while in between two adjacent peaks $\Delta\rho(E)$ becomes negative in agreement with the recently demonstrated sum rule for $\Delta\rho(E)$.⁹

Interesting features are found when comparing $\Delta\rho(E)$ for different thicknesses of the AlAs barriers; Figs. 2(a), 2(b), and 2(c) show the calculated $\Delta\rho(E)$ for 0, 1, and 2 ML's of AlAs, respectively (0 ML refers to standard $\text{Al}_{0.3}\text{Ga}_{0.7}\text{As}/\text{GaAs}$ QW's). It is found that the peaks in $\Delta\rho(E)$ become sharper and higher when increasing the AlAs barrier thickness, the resonances approaching true bound states for infinite barriers. It is also worth stressing that, due to the wave-function reflection at the well interfaces, the resonances in $\Delta\rho(E)$ are present even in the 0-ML structure; nevertheless, they are much broader than in the DBQW case. In fact, the second resonance in $\Delta\rho(E)$ for the 0-ML sample is already less pronounced than the fifth resonance of both the 1- and 2-ML DBQW's. Therefore, one expects much weaker signatures, if any at all, of the quasibound states in the optical spectra of the 0-ML structures (i.e., standard QW's) with respect to the 1–2-ML DBQW's, particularly if one takes into account that several mechanisms, such as, for example, fluctuations in the layer thickness, phonon interaction, and alloy disorder, contribute to smear out the resonances in the continuous spectrum of real samples.

Similar calculations of $\Delta\rho(E)$ have been performed for the holes, assuming parabolic bands and neglecting the complicated band dispersion. We find that, due to the larger effective mass of the holes compared to the elec-

trons, the resonances become denser. A summary of the quasibound-state energies for electrons and holes is reported in Table I for the 1- and 2-ML DBQW's investigated.

Finally we remark that the value of the well thickness modifies slightly the energy position of the quasibound states inside the barrier region, due to interference with the wave function reflected at the second AlAs layers. Therefore, since our samples have three wells of different widths separated by identical $\text{Al}_{0.3}\text{Ga}_{0.7}\text{As}$ barriers, two nearly degenerate resonances are found. They correspond to quasibound states localized in the two $\text{Al}_{0.3}\text{Ga}_{0.7}\text{As}$ barriers between the wells, respectively. However, the difference between their energy positions is so small that they cannot be resolved in real samples; the values reported in Table I correspond to the arithmetic average of the two values.

III. SAMPLES AND EXPERIMENTS

Three samples have been used in this work: two DBQW heterostructures with one and two AlAs ML's at each side of the GaAs QW (hereafter labeled 1 ML and 2 ML, respectively) and a reference sample, labeled 0 ML, with isolated standard GaAs/ $\text{Al}_{0.3}\text{Ga}_{0.7}\text{As}$ single-quantum-well (SQW) structures. All samples have been grown by molecular-beam epitaxy (MBE) under similar conditions; details of the growth procedure can be found in Ref. 13. Each structure contains three QW's with nominal thicknesses of 80, 40, and 20 Å, grown in this sequence from the buffer layer; 500-Å-thick layers of $\text{Al}_{0.3}\text{Ga}_{0.7}\text{As}$ separate from each other the QW regions, as shown in Fig. 1.

The photoluminescence (PL) spectra have been performed using, as excitation, the 5145-Å line of an Ar^+ laser; PLE spectra of the samples around the energy of the $\text{Al}_{0.3}\text{Ga}_{0.7}\text{As}$ band gap have been obtained using an Ar^+ -pumped dye laser tunable in the wavelength interval 6200–6700 Å. In both cases, the PL signal was dispersed by a double grating monochromator and detected by usual phonon-counting techniques. A Nd:YAG (yttrium aluminum garnet) synchronously pumped dye laser, operating in the same wavelength range (6200–6700 Å), has been used for excitation in the TRPL measurements; the time duration of the laser pulses was 3 ps with a re-

TABLE I. Energies of the first five electron (E_e) and hole (E_h) quasibound states, from the calculation of $\Delta\rho(E)$, referred to the bottom of the conduction band or the top of the valence band of the $\text{Al}_{0.3}\text{Ga}_{0.7}\text{As}$ barriers, respectively, in the multi-DBQW structures investigated. The quantity $\Delta_{eh}(n \rightarrow 1)$ is the energy separation of the n th $\Delta n = 0$ transition with respect to the first one, that is, $\Delta_{eh}(n \rightarrow 1) = [E_e(n) + E_h(n)] - [E_e(1) + E_h(1)]$. The PLE experimental values are an average of the 20-, 40-, and 80-Å DBQW data. The values from the reflectivity spectra come from the positions of the minima.

Level n	E_e (meV)	E_h (meV)	1 ML $\Delta_{eh}(n \rightarrow 1)$ (meV)		E_e (meV)	E_h (meV)	2 ML $\Delta_{eh}(n \rightarrow 1)$ (meV)	
			Calculated	Experimental			Calculated	Experimental
1	1.61	0.325		PLE Reflect.	1.52	0.325		PLE Reflect.
2	6.4	1.30	5.8	5.5–6	6.06	1.310	5.5	4.6–5.5
3	14.3	2.92	15.3	16–15	13.6	2.94	14.7	16–13
4	25.2	5.17	28.5	30–27	24.0	5.21	27.4	30–26
5	39.2	8.05	45.4	–43	37.2	8.12	43.5	–42

petition rate of 76 MHz. The PL decay has been recorded by a streak camera operating in synchroscan mode with an overall temporal resolution of the order of 20 ps. The TRPL experiments consisted in measuring, for all samples, the time evolution of the PL signal from the lowest excitonic transition in each QW as a function of the excitation energy (time-resolved PLE) around the band-gap energy of the $\text{Al}_{0.3}\text{Ga}_{0.7}\text{As}$ barriers (energy resolution of about 1 meV).

Reflectivity measurements have been performed at normal incidence, by using a beam splitter at 45° between the incident light and the optical axis defined by the sample and the entrance slit of the monochromator. Reflected light from the cryostat windows has been removed from the optical axis by slightly rotating the cryostat head. The white light was obtained from a tungsten lamp, collimated on a diffusive sheet and transformed into a parallel beam of 8 mm diam. The beam has been focused onto the sample surface with a spot size of about 1 mm diam. The reflected light was dispersed by the double grating monochromator and analyzed by standard photon-counting detection.

All measurements have been carried out at liquid-helium temperature with an excitation sheet density of the order of 10^9 cm^{-2} .

IV. RESULTS AND DISCUSSION

In Fig. 3 the PL spectra of the three samples (0, 1, and 2 ML) in the energy range investigated are reported. The most striking feature in the PL spectra is the blueshift of the excitonic transitions within the QW's when inserting the AlAs ML's, the greater the thinner the well width, in agreement with the calculated subband energies from a simple effective-mass model.^{1,13} It is worth noting that the PL integrated intensity turns out to be of the same order in all the QW's investigated, even in the case of the 20-Å DBQW's, in spite of the shallowness of their electron subbands.^{1,2}

The PL lines around 1.96–1.97 eV in the 1- and 2-ML

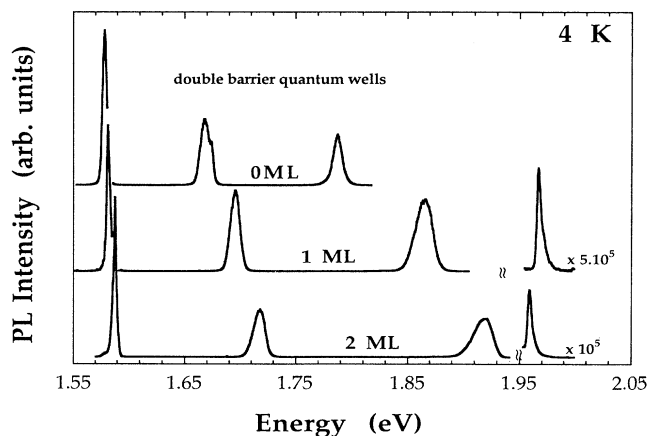


FIG. 3. PL spectra for all the samples investigated. The intensity of the above-barrier PL lines has been multiplied by the scale factor reported.

samples come from recombination in the $\text{Al}_{0.3}\text{Ga}_{0.7}\text{As}$ barriers and are extremely weak (note the change of scale) if compared with the excitonic transitions inside the QW's. No PL signal from the barriers has been detected in the 0-ML sample, suggesting a very fast and efficient carrier capture into the quantum wells. Note also that the recombination band from the barriers of the 2-ML sample is more intense than that of the 1-ML sample, in qualitative agreement with the localization enhancement predicted in Sec. II when increasing the number of AlAs layers.

We report in Fig. 4(a) a comparison of reflectivity spectra for the 0- and 1-ML samples in the energy range of interest, namely, around the $\text{Al}_{0.3}\text{Ga}_{0.7}\text{As}$ band gap. A striking difference is immediately seen between the two spectra: while only the usual resonance at the alloy absorption edge is observed in the 0-ML sample, a much more complicated structure is found in the case of the 1-ML DBQW's; similar features have been retrieved in the 2-ML structure as well. This oscillatory behavior of the reflectivity spectrum of the 1- and 2-ML structures, at energies higher than the $\text{Al}_{0.3}\text{Ga}_{0.7}\text{As}$ band gap, is very likely due to the existence of the quasibound states discussed in the preceding section. However, a line-shape analysis of the reflectivity spectra of complex structures such as the 1- or 2-ML samples is quite complicated and outside the aim of this paper.

More direct evidence of the existence of quasibound states above the $\text{Al}_{0.3}\text{Ga}_{0.7}\text{As}$ barrier energy has been obtained by means of PLE techniques. In Fig. 4(b), PLE spectra of the 40-Å well for the 1- and 2-ML samples are reported for excitation energy around the $\text{Al}_{0.3}\text{Ga}_{0.7}\text{As}$

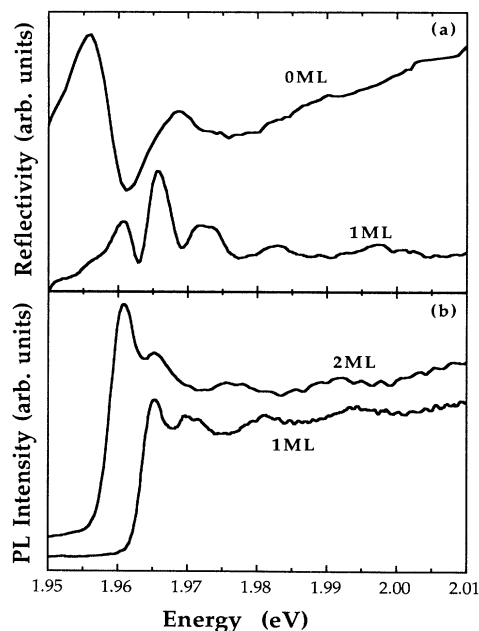


FIG. 4. (a) Reflectivity spectra of the 0- and 2-ML samples in the energy region around the $\text{Al}_{0.3}\text{Ga}_{0.7}\text{As}$ band-gap energy. (b) PLE spectra of the 1- and 2-ML samples in the same energy range.

band gap. A series of peaks, at energies higher than the absorption edge of the $\text{Al}_{0.3}\text{Ga}_{0.7}\text{As}$ barriers, is observed. As shown by a comparison with Fig. 4(a), they correspond to the resonances found in the reflectivity spectra. It is also worth noting that in the PLE spectrum of the 0-ML sample we only observe a single peak at the $\text{Al}_{0.3}\text{Ga}_{0.7}\text{As}$ absorption edge.

The energy of the peaks in the optical spectra can be directly compared with the predictions of the model discussed above. In fact, due to the close matching between the resonances in $\Delta\rho(E)$ and the true bound states in an infinitely deep well demonstrated in Sec. II, we can assume that only transitions between corresponding quasibound states are allowed in these structures. Each peak in the PLE spectra is therefore assigned to a $\Delta n = 0$ transition. However, given the well-known uncertainties in calibrating the Al content in the alloy composition and in the x dependence of the $\text{Al}_x\text{Ga}_{1-x}\text{As}$ band-gap energy, we believe it is more reliable to use the energy separation of the transitions with respect to the first resonance. They are reported in Table I for both the PLE and the reflectivity measurements (assuming the minima of the structures in the reflectivity spectra as a reference for the

energy positions) in addition to the corresponding energies of the quasibound states found in $\Delta\rho(E)$. The comparison shows a very good agreement between the experimental data and the theoretical predictions, thus demonstrating both the presence of the quasibound states and the related increase of the optical absorption in the 3D continuum.

We would like to remark that the structures observed in the optical spectra of the DBQW's, even if clearly resolved, are extremely weak and broad if compared with the resonances in $\Delta\rho(E)$ found in Sec. II. As already discussed, several mechanisms are effective in smearing out the resonances in the continuous spectrum of a real sample. This is very likely the reason that we do not observe, in the 0-ML sample, any particular structure associated to the series of resonances in $\Delta\rho(E)$; they are, in fact, much broader than the corresponding ones in the 1- and 2-ML DBQW samples.

The presence of resonances localized in the $\text{Al}_{0.3}\text{Ga}_{0.7}\text{As}$ region should also manifest itself in a variation of the carrier capture time into the well, as suggested by the PL recombination from the $\text{Al}_{0.3}\text{Ga}_{0.7}\text{As}$ barrier observed in the 1- and 2-ML samples. Figure 5(a) shows the PL decay curves of the 40-Å DBQW in the 2-ML sample for two different excitation energies (solid lines), together with the laser pulse (dashed line) used as a reference in order to have a reliable time origin. The lower curve corresponds to the time evolution of the PL signal for excitation of the carriers within the well ($E_{\text{exc}} = 1.894$ eV), while the upper curve ($E_{\text{exc}} = 1.962$ eV) corresponds to carrier excitation at the $\text{Al}_{0.3}\text{Ga}_{0.7}\text{As}$ barrier, around the energy of the first resonant state. Defining the PL rise time as the time at which the PL intensity is maximum, a significant difference of the order of about 45 ps is observed in the PL rise times between below- and above-barrier excitation.

The excitation energy dependence of the PL rise time, as defined above, is reported in Fig. 5(b) for the 40-Å well of the three samples. A sharp increase of the rise time is observed in the 1- and 2-ML samples when exciting at the $\text{Al}_{0.3}\text{Ga}_{0.7}\text{As}$ band gap, while a nearly constant PL rise time is found in the reference sample (0 ML). A similar behavior is observed in the other wells, even if the differences between the PL rise time below and above barrier are somehow less pronounced.

Since the PL decay time is found to be constant, independent of the excitation energy, the variations of the PL rise time shown in Fig. 5(b) are very likely due to a change in the capture efficiency. In fact, for an excitation above the $\text{Al}_{0.3}\text{Ga}_{0.7}\text{As}$ band gap the carriers are mainly photogenerated in the barrier regions and have to be trapped inside the QW's before they recombine. Moreover, the capture probability depends on the overlap between the carrier wave functions of the bound and unbound states. At the same time, the quasibound states induced by the insertion of the AlAs layers in the DBQW's are strongly localized in the barrier regions. We therefore attribute the observed increase in the PL rise time to a reduction of the capture efficiency due to the presence of quasibound states localized in the $\text{Al}_{0.3}\text{Ga}_{0.7}\text{As}$ barriers.

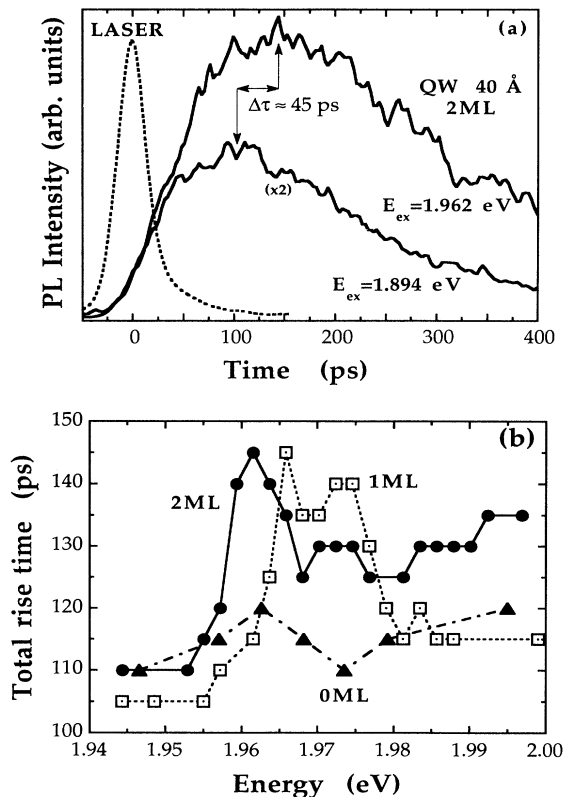


FIG. 5. (a) PL decay curves of the 40-Å QW, 2-ML sample, for two different excitation energies: inside the QW (lower curve, $E_{\text{exc}} = 1.894$ eV) and around the energy of the first above-barrier resonant state (upper curve, $E_{\text{exc}} = 1.962$ eV). The dashed line corresponds to the laser pulse which marks the time origin. (b) PL rise time as a function of the excitation energy for the 40-Å QW in the 0-, 1-, and 2-ML samples; the lines are only guides to the eye.

V. CONCLUSIONS

We have reported an experimental analysis of the above-barrier transitions in $\text{Al}_{0.3}\text{Ga}_{0.7}\text{As}/\text{AlAs}/\text{GaAs}$ DBQW structures using both continuous-wave and time-resolved PL techniques in addition to reflectivity measurements. The series of peaks at energies above the $\text{Al}_{0.3}\text{Ga}_{0.7}\text{As}$ band gap observed in the optical spectra agree fairly well with the resonances found in the density of states of the DBQW continuous spectrum, clearly demonstrating the existence of quasibound states localized in the barrier regions.

We believe that the observed increase in the PL rise time for resonant excitation above the $\text{Al}_{0.3}\text{Ga}_{0.7}\text{As}$ barrier and the modifications in the carrier dynamics originated by the existence of such states might be of some relevance towards the realization of novel quantum-well devices.

ACKNOWLEDGMENTS

We wish to thank Dr. W. Trzeciakowski for helpful discussions and for providing us with the computational algorithm for DOS calculations; Professor F. Meseguer for the use of the facilities at the Raman laboratory of the ICMU-UAM (Madrid); Dr. J. Massies and Dr. C. Deparis for providing the samples. One of us (J.M.P.) acknowledges financial support from the Conselleria de Cultura, Educació i Ciència de la Generalitat de València and from the Spanish Ministerio de Educación y Ciencia.

APPENDIX

In this appendix we briefly derive, for the sake of completeness, the method used in Sec. II for determining $\Delta\rho(E)$; we refer to previous publications^{11,12} for a more detailed discussion. We consider the heterostructure inside a large, but finite, box of dimension L_B so that the energy spectrum is dense but discrete. The DOS of the empty box $\rho_0(E)$ and the DOS of the system with the het-

erostructure $\rho(E)$ are then defined as

$$\rho_0(E_n^0) = \frac{1}{\Delta_n^0}, \quad (\text{A1})$$

$$\rho(E_n) = \frac{1}{\Delta_n}, \quad (\text{A2})$$

where $\Delta_n^0 = E_{n+1}^0 - E_n^0$ and $\Delta_n = E_{n+1} - E_n$ are the spacings between the levels. These are given by the eigenvalue conditions

$$D_0(E_n^0) = 0, \quad (\text{A3})$$

$$D(E_n) = 0 \quad (\text{A4})$$

for the empty box and for the box with the structure, respectively. In the limit of the large box we have

$$\Delta_n = \Delta_n^0 + x_n, \quad (\text{A5})$$

with $|x_n| \ll \Delta_n^0$, from which the change in the DOS $\Delta\rho(E) = \rho(E) - \rho_0(E)$ becomes

$$\Delta\rho(E_n) \cong -\frac{x_n}{(\Delta_n^0)^2} \cong \frac{1}{(\Delta_n^0)^2} \frac{D(E_n + \Delta_n^0)}{D'(E_n + \Delta_n^0)}, \quad (\text{A6})$$

where $D'(E)$ is the first derivative of $D(E)$. Therefore, knowing the conditions (A3) and (A4) for the energy levels, we can easily determine $\Delta\rho(E)$.

A tricky aspect of the outlined method is that the levels must be split into different classes, depending on the unperturbed wave-function phase at the heterostructure position.¹¹ To the i th class corresponds a separated sub-density of states $\Delta\rho_i(E)$ which has to be evaluated with the described method; the total $\Delta\rho(E)$ is the sum of $\Delta\rho_i(E)$. For example, setting the heterostructure in the middle of the box, there are two classes corresponding to even and odd wave functions. The reason is essentially that the infinite system ($L_B \rightarrow \infty$), for which $\Delta\rho(E)$ is defined by Eq. (1), is twofold degenerate while the finite system is nondegenerate.¹⁰

*Permanent address: Departament de Física Aplicada, Universitat de València, 46100 Burjassot, València, Spain.

¹J. Martinez-Pastor, M. Gurioli, M. Colocci, C. Deparis, B. Chastaingt, and J. Massies, Phys. Rev. B **46**, 2239 (1992).

²M. Gurioli, J. Martinez-Pastor, M. Colocci, C. Deparis, B. Chastaingt, and J. Massies, Phys. Rev. B **46**, 6922 (1992).

³M. Leroux, N. Grandjean, B. Chastaingt, C. Deparis, and J. Massies, Phys. Rev. B **45**, 11 846 (1992).

⁴B. F. Levine, K. K. Choi, C. G. Bethea, J. Walker, and R. J. Malik, J. Appl. Phys. **50**, 1092 (1987).

⁵B. F. Levine, C. G. Bethea, K. K. Choi, J. Walker, and R. J. Malik, J. Appl. Phys. **64**, 1591 (1988).

⁶D. Dossa, L. C. Lew Yan Voon, L. R. Ram-Mohan, C. Parks, R. G. Alonso, A. K. Ramdas, and M. R. Melloch, Appl. Phys. Lett. **59**, 2706 (1991).

⁷H. Schneider, F. Fuchs, B. Dischler, J. D. Ralston, and P. Koidl, Appl. Phys. Lett. **58**, 2234 (1991).

⁸M. S. Kiledjian, J. N. Schulman, and K. L. Wang, Phys. Rev. B **44**, 5616 (1991).

⁹W. Trzeciakowski and M. Gurioli, J. Phys. Condens. Matter **5**, 105 (1993).

¹⁰W. Trzeciakowski and M. Gurioli, J. Phys. Condens. Matter **5**, 1701 (1993).

¹¹W. Trzeciakowski, D. Sahu, and T. F. George, Phys. Rev. B **40**, 6058 (1989).

¹²W. Trzeciakowski and M. Gurioli, Phys. Rev. B **44**, 3880 (1991).

¹³Y. Chen, G. Neu, C. Deparis, and J. Massies, Appl. Phys. Lett. **58**, 2111 (1991).